Low-Temperature Stabilization of Tetragonal Zirconia by Bismuth

Antonino Gulino,* Salvatore La Delfa, and Ignazio Fragalà*

Dipartimento di Scienze Chimiche Università di Catania, V. le A. Doria 6, 95125, Catania Italy

Russell G. Egdell*

Inorganic Chemistry Laboratory, South Parks Road, Oxford OX1 3QR, UK

Received December 4, 1995. Revised Manuscript Received March 5, 1996[⊗]

Low-temperature (400−800 °C) stabilization of tetragonal zirconia, prepared by a hydroxide gel route and low-temperature annealing, has been achieved by partial substitution of Zr^{4+} with Bi^{3+}. XRD and Raman spectroscopy have been used for characterization of the doped zirconia powders as well as for identification of the crystal symmetry. XPS data provide evidence of the presence of Bi(III) and of a small amount of a lower Bi sub-oxide. A phase transition from the tetragonal structure of zirconia to the monoclinic phase takes place above 800 °C. The grain size dependence upon the annealing temperature has been evaluated using the Scherrer equation. Particle morphology and size have been directly imaged with the aid of SEM.

Introduction

The polymorphism of ZrO_2 still represents an intriguing area. Monoclinic ZrO_2 is based on 7-coordinate Zr^{4+} ions, but it transforms to a tetragonal polymorph around 1100 °C. A tetragonal to cubic transition is observed around 2300 °C.[1] The transition at 1100 °C restricts the use of the pure oxide as a refractory material.[1] At room temperature only the monoclinic form is thermodynamically stable.[2−6]

Although there have been reports on the formation and stability of tetragonal[7−9] and cubic[10] zirconia thin films as well as on the stability of cubic phase in nanocrystalline ZrO_2,[11] most effort has been devoted to stabilization of zirconia into tetragonal or, even better, into cubic phases by using various aliovalent cation dopants. They are believed to substitute for the Zr^{4+} ion in the cation framework, thus creating oxygen vacancies due to charge compensation.[12−16] Partially stabilized tetragonal and fully stabilized cubic zirconia have attracted considerable attention because these solid solutions possess remarkable physicochemical properties which, in turn, have stimulated their applications as oxygen sensors, fuel cells, catalysts, and other interesting applications.[17−26] Moreover they represent good toughening agents because of their excellent mechanical properties.[2]

The factors governing the stability of doped stabilized zirconia were first investigated in 1924.[27] Nevertheless several aspects concerning the dopant prerequisites needed to stabilize the high-temperature polymorphs remain unclear. A model has been proposed setting out criteria for suitable dopant cations.[28] In particular stabilizing cations must have larger ionic sizes, a lower formal charge state, and a higher ionicity than Zr.[28] Although there is some experimental support for the

[⊗] Abstract published in *Advance ACS Abstracts,* May 1, 1996.

(1) Wells, A. F. *Structural Inorganic Chemistry 4*; Clarendon Press: Oxford, 1975.
(2) Li, P.; Chen, I.-W.; Penner-Hahn, J. E. *Phys. Rev. B* **1993**, *48*, 10063.
(3) Li, P.; Chen, I.-W.; Penner-Hahn, J. E. *Phys. Rev. B* **1993**, *48*, 10074.
(4) Li, P.; Chen, I.-W.; Penner-Hahn, J. E. *Phys. Rev. B* **1993**, *48*, 10082.
(5) Sergo, V.; Schmid, C.; Meriani, S.; Evans, A. G. *J. Am. Ceram. Soc.* **1994**, *77*, 2971.
(6) Ishida, K.; Hirota, K.; Yamaguchi, O.; Kume, H.; Inamura, S.; Miyamoto, H. *J. Am. Ceram. Soc.* **1994**, *77*, 1391.
(7) Gould, B. J.; Povey, I. M.; Pemble, M. E.; Flavell, W. R. *J. Mater. Chem.* **1994**, *4*, 1815 and references therein.
(8) Hwang, C. S.; Kim, H. J. *J. Mater. Res.* **1993**, *8*, 1361.
(9) Scanlan, C. M.; Gajdardziska-Josifovska, M.; Aita, C. R. *Appl. Phys. Lett.* **1994**, *64*, 3548 and references therein.
(10) Xue, Z.; Vaartstra, B. A.; Caulton, K. G.; Chisholm, M. H. *Eur. J. Solid State Inorg. Chem.* **1992**, *29*, 213 and references therein.
(11) Chatterjee, A.; Pradhan, S. K.; Datta, A.; De, M.; Chakravorty, D. *J. Mater. Res.* **1994**, *9*, 263 and references therein.
(12) Li, P.; Chen, I.-W.; Penner-Hahn, J. E. *J. Am. Ceram. Soc.* **1994**, *77*, 118.
(13) Xue, J.; Dieckmann, R. *Solid State Ionics* **1994**, *73*, 273.
(14) Fukuya, M.; Hirota, K.; Yamaguchi, O.; Kume, H.; Inamura, S.; Miyamoto, H.; Shiokawa, N.; Shikata, R. *Mater. Res. Bull.* **1994**, *29*, 619.
(15) Chen, S.; Deng, W.; Shen, P. *Mater. Sci. Eng. B* **1994**, *22*, 247.
(16) Boutz, M. M. R.; Winnubst, A. J. A.; Hartgers, F.; Burggraaf, A. J. *J. Mater. Sci.* **1994**, *29*, 5374.
(17) Etsell, T. H.; Flengas, S. N. *Chem. Rev.* **1970**, *70*, 1970.
(18) Sasaki, K.; Seifert, H. P.; Gauckler, L. J. *J. Electrochem. Soc.* **1994**, *141*, 2759.
(19) Yamamoto, O.; Arati, Y.; Takeda, Y.; Imanishi, N.; Mizutani, Y.; Kawai, M.; Nakamura, Y. *Solid State Ionics* **1995**, *79*, 137.
(20) Van Herle, J.; McEvoy, A. J.; Ravindranathan Thampi, K. *J. Mater. Sci.* **1994**, *29*, 3691.
(21) Kurosawa, H.; Yan, Y.; Miura, N.; Yamazoe, N. *Chem. Lett.* **1994**, 1733.
(22) Cao, G. Z. *J. Appl. Electrochem.* **1994**, *24*, 1222.
(23) Otsuka, K.; Ando, T.; Suprapto, S.; Wang, Y.; Ebitani, K.; Yamanaka, I. *Catal. Today* **1994**, *24*, 315.
(24) Garvie, R. S.; Hannink, R. H.; Pascoe, R. T. *Nature* **1975**, *258*, 703.
(25) Fischer, G. *Ceram. Bull.* **1986**, *65*, 1355.
(26) Yokoyama, T.; Setoyama, T.; Fumita, N.; Nakajima, M.; Maki, T.; Fuji, K. *Appl. Catal.* **1992**, *88*, 149.
(27) Van Arkel, E. A. *Physica* **1924**, *4*, 286.
(28) Ho, S. M. *Mater. Sci. Eng.* **1982**, *54*, 23.

S0897-4756(95)00558-8 CCC: $12.00

above model,[29−31] other data remain not clear. First, there is evidence that undersized dopants may stabilize the tetragonal form of ZrO_2.[12] Second, ZrO_2 can be stabilized by some tetravalent cations[12−15] which do not introduce oxygen vacancies. Finally ZrO_2 has been stabilized using cations which are less ionic than Zr.[2−5,12,32]

In the present investigation we report on the low-temperature stabilization of the novel Bi^{3+}-doped ZrO_2 using a coprecipitation method. Present results are of relevance in the perspective of the ZrO_2 fabrication for several catalytic applications since, low annealing temperatures are required in order to obtain higher area surfaces.[32−33]

Experimental Details

The 3%, 5%, 7%, 10%, and 15% Bi-doped ZrO_2 samples were synthesized by a coprecipitation method using high-purity zirconyl chloride hydrate (99.99% Aldrich) and bismuth(III) oxide (99.99% Aldrich). Appropriate quantities of the starting materials were separately dissolved in water ($ZrOCl_2$) and in concentrated HCl (Bi_2O_3). The solutions were mixed and, under continuous stirring, neutralized with concentrated NH_3 solution to pH = 10. The hydroxide gels thus formed were filtered off, washed with distilled water, and dried at 90 °C. The resulting powders were fired for 4 h[12] at different temperatures (200, 300, 400, 500, 600, 700, 800, and 1000 °C) in recrystallized alumina crucibles. Care was taken to avoid Si-containing crucibles which contaminate the Bi_2O_3 oxide.[1] A sample of undoped ZrO_2 was prepared by a similar procedure but without addition of Bi dopant. All the final samples were white with the exception of the 1000 °C annealed powders which were yellow.

X-ray powder diffraction (XRD) data were recorded on a computer-interfaced Philips PW 1130 diffractometer operating in a Bragg−Brentano geometry (Cu Kα radiation 20 mA and 40 kV) over a $20° < 2\theta < 80°$ angular range.

Raman spectra were taken at 300 K in the 90° geometry, with 100 mW of the 496.5 nm line of an Ar^+ laser using a Jobin Yvon U1000 spectrometer. The instrumental resolution was 4 cm^{-1}.

The Bi-doping levels of samples fired up to 1000 °C were established by titrimetry[34] after fusion of the samples with Na_2O_2 + NaOH in nickel crucibles and by examination of Zr Kβ and Bi Lγ emission, using a Philips PW 1410/00/60 wavelength-dispersive X-ray fluorescence spectrometer, equipped with a tungsten anode and a LiF 220 crystal as secondary radiation-dispersive element.[35] Samples for X-ray fluorescence analysis were prepared as already described.[36] Bi contents were close to the nominal doping levels in all cases, but the 1000 °C annealed samples showed a 7% decrease in Bi content below nominal levels. This shows that there is negligible volatilization of Bi oxides during the firing procedures.

Sample powders for XPS measurements were pressed into pellets (10 tons) between tungsten carbide dies and fired for 4 h in recrystallized alumina boats. Samples were mounted on Mo stubs and held in position with Mo wires. Additional XPS measurements were performed directly on sample powders held on indium foil. No spectral differences were detected. All

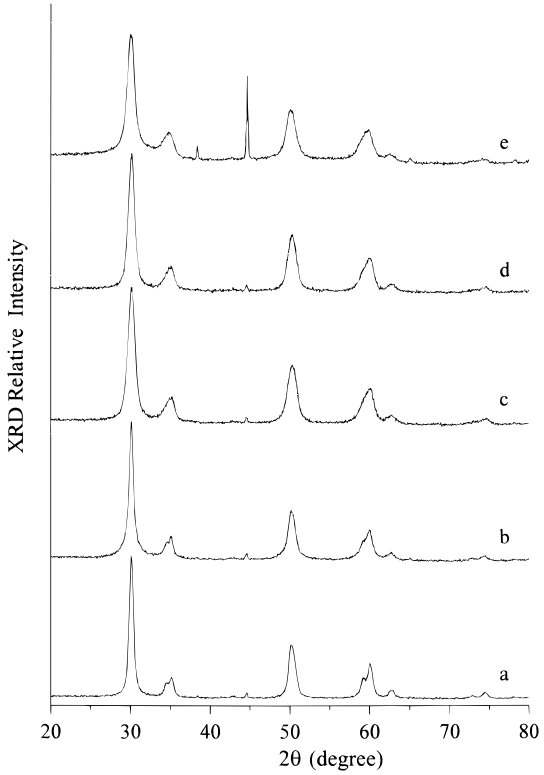

Figure 1. X-ray powder diffraction patterns, over a $20° < 2\theta < 80°$ angular range, for 3% Bi-doped ZrO_2 (a); 5% Bi-doped ZrO_2 (b); 7% Bi-doped ZrO_2 (c); 10% Bi-doped ZrO_2 (d), and 15% Bi-doped ZrO_2 (e) solid solutions fired at 400 °C. Peaks at $2\theta = 38.47$, $2\theta = 44.73$, and $2\theta = 65.13$ are due to the Al sample holder.

XPS measurements were made with a PHI 5600 Multi Technique System (base pressure of the main chamber 3×10^{-10} Torr). The nominal analyzer resolution was set to 400 meV. Spectra were excited with Al Kα radiation. Structure due to satellite radiation has been subtracted from the spectra before the data processing. The XPS peak intensities were obtained after Shirley background removal.[37] Corrections for the energy shift, due to the steady-state charging effect, were accomplished by assuming 284.6 eV binding energy (BE) for the C 1s peak, due to adventitious carbon contamination.[38]

Additional analyses of sample surfaces were carried out by scanning electron microscopy (SEM) using a 20 keV electron beam and a resolution better than 0.2 μm.

Results and Discussion

Undoped ZrO_2 materials were first investigated as reference. At temperatures lower than 500 °C they are amorphous. At 500 °C some evidence of crystalline phases are present in terms of monoclinic and less intense tetragonal XRD reflections. At higher firing temperatures the tetragonal lines become weaker and at 800 °C samples are completely monoclinic (Figure S1).

The Bi-doped samples annealed up to 300 °C are amorphous. Above 300 °C, broad peaks, corresponding to the formation of a crystalline phase, begin to appear. The crystallization is completed at 400 °C. The X-ray diffraction patterns of the 3%, 5%, 7%, 10%, and 15% Bi-doped ZrO_2 samples, fired at 400 °C, are shown in Figure 1. All of the XRD patterns of the low-tempera-

(29) Yoshimura, M. *Am. Ceram. Soc. Bull.* **1988**, *67*, 1950.
(30) Dexpert-Ghys, J.; Faucher, M.; Caro, P. *J. Solid State Chem.* **1984**, *54*, 179.
(31) Allpress, J. G.; Rossell, H. J. *J. Solid State Chem.* **1975**, *15*, 68.
(32) Keshavaraja, A.; Ramaswamy, A. V. *J. Mater. Res.* **1994**, *9*, 837 and references therein.
(33) Afanasiev, P.; Geantet, C.; Breysse, M. *J. Catal.* **1995**, *153*, 17.
(34) Bishop, E. *Indicators*; Pergamon: Oxford, 1972.
(35) Condorelli, G. G.; Malandrino, G.; Fragalà, I. *Chem. Mater.* **1994**, *6*, 1861.
(36) Hutchison, C. S. *Laboratory Handbook of Petrographic Techniques*; Wiley: New York, 1974.
(37) Repoux, M. *Surf. Interface Anal.* **1992**, *18*, 567.
(38) Ingo, G. M. *Appl. Surf. Sci.* **1993**, *70/71*, 235.

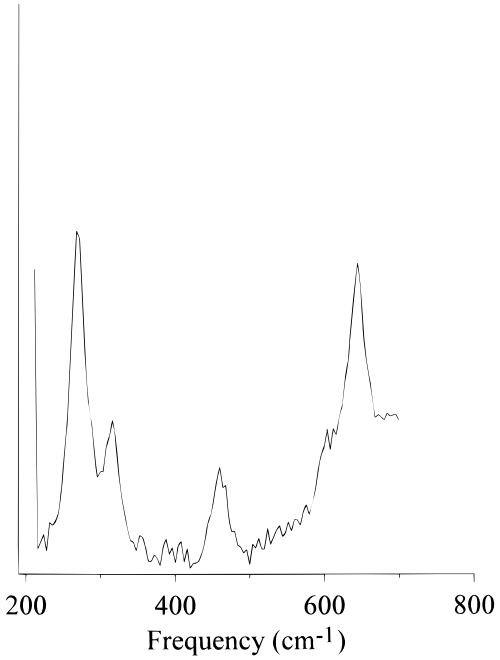

Figure 2. Representative Raman spectrum of the 10% Bi-doped ZrO_2 solid solution fired at 400 °C and measured in the 200−700 cm^{-1} frequency region.

Table 1. Space Groups and Raman-Active Bands of ZrO_2 Polymorphs

space group	phase	no. of Raman-active bands
$C^5_{2h}(P2_1/C)$	monoclinic	18
$D^{15}_{4h}(P4_2/nmc)$	tetragonal	6
$O^5_h(Fm^3m)$	cubic	1

ture (400−800 °C) calcinated powders show a similar set of broadened peaks but no evidence for the monoclinic phase. The presently observed XRD broadening, already detected in other stabilized ZrO_2 systems,[12] precludes a straightforward interpretation of the XRD pattern since most of the reflections of cubic and tetragonal zirconia overlap.[11] It has been reported that slight variations in the lattice constants ($a = b \neq c$) of tetragonal zirconia give rise to characteristic tetragonal line splittings. This splitting is, by contrast, absent in the cubic structure.[39] The distinct splitting of the lines at $2\theta \cong 35°$ and $2\theta \cong 60°$, observed in samples having Bi contents lower than 7% (Figure 1a,b), therefore represents an indication of the tetragonal nature of these Bi-doped zirconia. Samples having Bi contents ≥7% do not show clear line splittings even though the lines at $2\theta \cong 35°$ and $2\theta \cong 60°$ remain asymmetric (Figure 1c,e). An unambiguous phase assignment certainly requires additional supporting evidence, and the Raman spectroscopy provides another method for the identification of crystal symmetry in zirconia polymorphs.[39−41]

The number of Raman-active bands of a zirconia crystal phase can be obtained from a factor analysis of the space groups of various polymorphs (Table 1).[39] The Raman spectra for the present (3−15%) Bi-doped samples

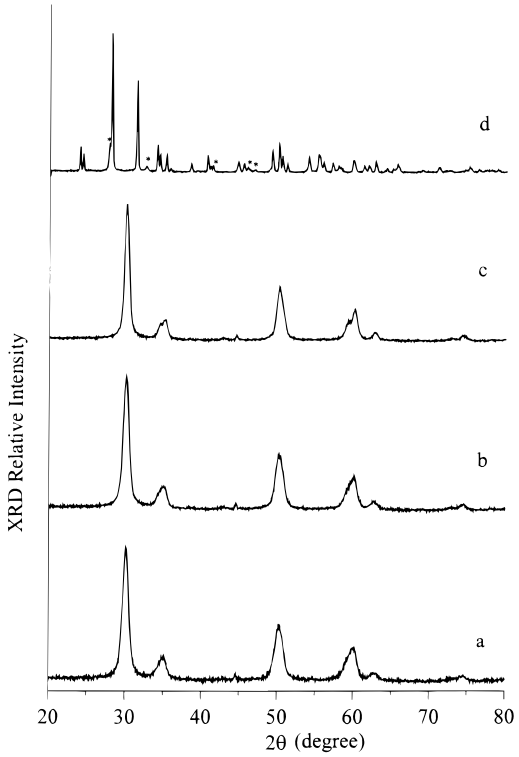

Figure 3. X-ray powder diffraction patterns, over a $20° < 2\theta < 80°$ angular range, for 10% Bi-doped ZrO_2 solid solutions fired at 400 (a), 600 (b), 800 (c), and 1000 °C (d). Peaks at $2\theta = 38.47$, $2\theta = 44.73$, and $2\theta = 65.13$ are due to the Al sample holder. Stars refer to Bi_2O_3.

(Figure 2) closely resemble those previously reported for Y-doped tetragonal zirconia[40,41] and point to a dominant tetragonal nature of the present Bi-doped samples. Nevertheless small amounts of cubic bismuth-doped zirconia cannot be ruled out.[40,41]

Upon increase of the temperature, the XRD lines of the 10% Bi-doped samples become sharper (Figure 3). In the 400−800 °C range they consist of a tetragonal phase. At 1000 °C 10% Bi-doped samples become monoclinic and XRD data show evidence of Bi_2O_3 (Figure 3d).[42−44] It, therefore, turns out that Bi is soluble enough in tetragonal zirconia up to 800 °C. Above this temperature, Bi_2O_3 separation occurs because its solubility in the ZrO_2 lattice has been exceeded under higher temperature treatments. A similar behavior has been already noticed in Fe_2O_3- and Ga_2O_3-doped zirconia.[12]

Particle sizes of the 10% Bi-doped sample at various temperatures were determined using XRD data and the Scherrer and Warren equations:[45]

$$S = 0.9\lambda/(B \cos \theta_B) \quad (1)$$

where S is the grain size of the crystallite, λ is the wavelength of the X-ray source, θ_B is the Bragg angle of the considered XRD peaks, and B represents the

(39) Srnivasan, R.; Simpson, S. F.; Harris, J. M.; Davis, B. H. *J. Mater. Sci. Lett.* **1991**, *10*, 352.
(40) Liu, D. W.; Perry, C. H.; Ingel, R. P. *J. Appl. Phys.* **1988**, *64*, 1413.
(41) Cai, J.; Raptis, Y. S.; Anastassakis, E. *Appl. Phys. Lett.* **1993**, *62*, 2781.
(42) Present data cannot be diagnostic either of the α-Bi_2O_3 or β-Bi_2O_3 because many of their XRD reflections overlap with the monoclinic zirconia lines.
(43) Tsubaki, M.; Koto, K. *Mater. Res. Bull.* **1984**, *19*, 1613.
(44) American Society for Testing and Material, Powder Diffraction Files (Joint Committee on Powder Diffraction Standards, USA, 1974), Set 1−5 (Revised), Inorganic.
(45) Warren, B. E. *X-ray Diffraction*; Addison-Wesley: Reading MA, 1969.

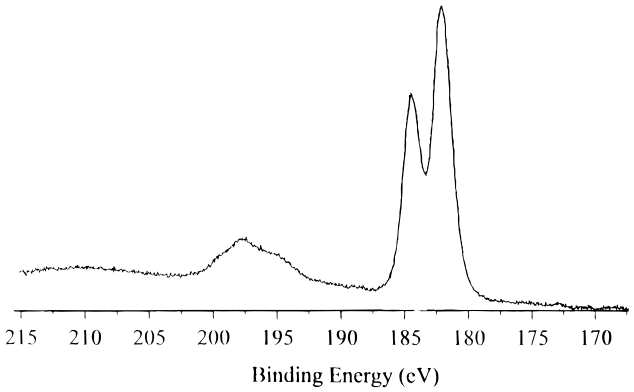

Figure 4. Al Kα excited XPS of 10% Bi-doped ZrO_2 solid solution fired at 400 °C and measured in the Zr 3d binding energy region. Structure due to satellite radiation has been subtracted from the spectra.

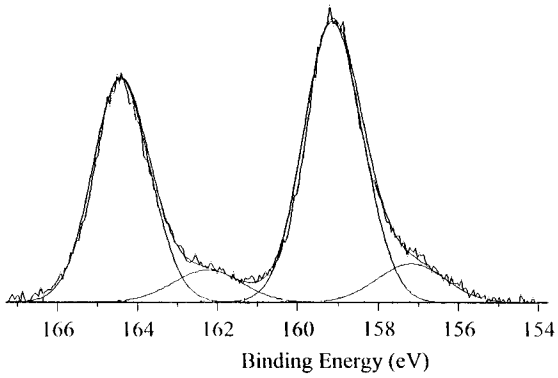

Figure 5. Al Kα excited XPS of 10% Bi-doped ZrO_2 solid solution fired at 400 °C and measured in the Bi 4f binding energy region. Structure due to satellite radiation has been subtracted from the spectra.

Table 2. Particle Sizes of 10% Bi-Doped ZrO_2 at Different Temperatures

firing temp (°C)	particle size (nm)	firing temp (°C)	particle size (nm)
400	7.0	700	11.3
500	7.6	800	19.7
600	8.4	1000	138.4

fwhm line broadening obtained as follows:

$$B^2 = B^2_{\mathrm{m}} - B^2_{\mathrm{s}}$$

where B^2_{m} is the fwhm line broadening of the material and B^2_{s} represents the fwhm line broadening of the internal standard (α-Al_2O_3). The resulting values of crystallite sizes, obtained from the (111) strongest reflections, are shown in Table 2. It is evident that higher temperature annealing results in the narrowing of the peaks (Figure 3) and, hence, in a grater grain growth (Table 2). A steady growth is observed below 800 °C. An abrupt increase is, by contrast, observed above this temperature where the transition to the monoclinic phase begins to be observed. Flavell et al. have observed a similar behavior in pure ZrO_2 thin films.[7]

Variations of XRD peak broadening is observed upon changing the Bi doping level. In particular peaks of 3% and 5% Bi-doped ZrO_2 are narrower than those with higher Bi contents (Figure 1), thus suggesting a difference in the related particle sizes. The presently found values of 13 nm for 3−5% doped samples and of 7 nm for the remaining 7%, 10%, and 15% doped samples suggest that high Bi contents retard grain growth.

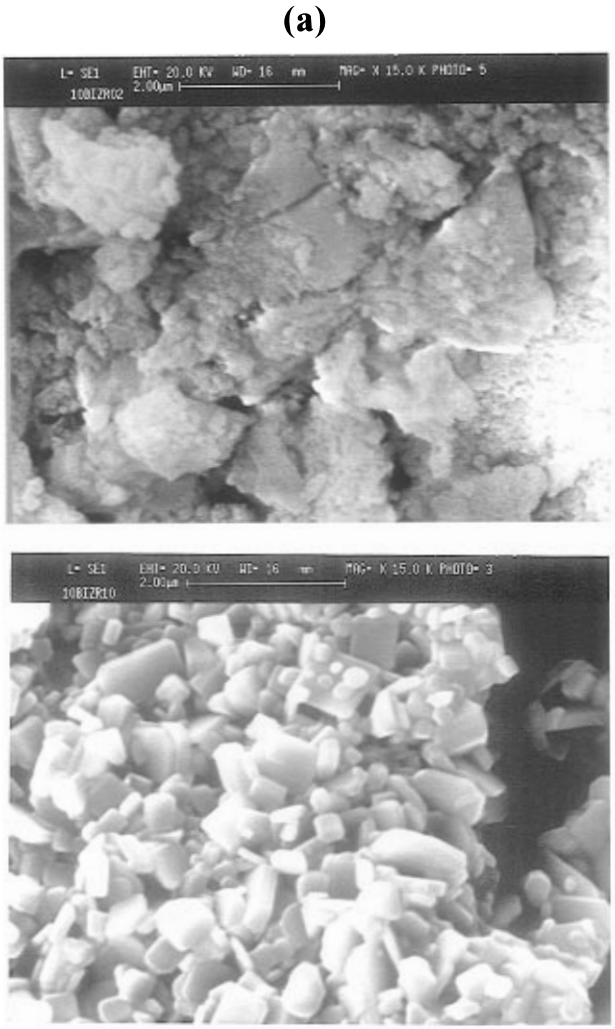

Figure 6. SEM images of 10% Bi-doped ZrO_2 solid solution as a function of the firing temperature: (a) 200 and (b) 1000 °C.

Moreover it is worthy of note that grain sizes of present tetragonal Bi-doped zirconia are similar to those found for cubic, pure nanocrystalline ZrO_2.[11]

Figure 4 shows the XPS spectrum of the 400 °C annealed 10% Bi-doped ZrO_2 in the Zr 3d energy region. Several interesting features are apparent: Zr 3d features consist of the main $3d_{5/2}$, $3d_{3/2}$ spin−orbit components at 181.89 and 184.24 eV, respectively.[46−48] Moreover, a satellite feature is found at about 15 eV from the main Zr $3d_{5/2}$ peak. In analogy to previous XPS results on pure and doped zirconia, this feature can be interpreted in terms of a shakeup phenomenon.[48] Interestingly, this satellite appears resolved into two 3d spin−orbit components.[49] The Bi 4f energy region of the same sample is shown in Figure 5. Asymmetries are clearly apparent in the low-binding-energy side of

(46) Majumdar, D.; Chatterjee, D. *J. Appl. Phys.* **1991**, *70*, 988.
(47) Sarma, D. D.; Rao, C. N. R. *J. Electron Spectrosc. Relat. Phenom.* **1980**, *20*, 25.
(48) Marletta, G.; Pignataro, S. *Chem. Phys. Lett.* **1986**, *124*, 414.
(49) This represents an experimental observation of possible spin−orbit feature associated to the shakeup structure of Zr 3d in ZrO_2. The study of shakeup phenomena of many stabilized zirconia is currently in progress.

the peaks. The energy position of the main peaks ($4f_{7/2}$ 159.2 eV, $4f_{5/2}$ 164.5 eV) and the spin−orbit splitting = 5.3 eV are in good agreement with those observed in a vacuum-deposited bismuth oxide film.[50,51] The energies associated with the lower BE components (157.3 and 162.4 eV) are evidence of a lower Bi oxidation state. On the basis of previously reported data,[50,51] they are consistent with the presence of BiO.

The XPS Bi 4f and Zr 3d peaks, taken at 45° emission relative to the surface plane, have been used to derive the effective surface Bi/Zr intensity ratios for the 10% Bi-doped sample, making due allowance for the relevant atomic sensitivity factors.[52] It is found that, at lower annealing temperatures (400−600 °C), the Bi/Zr intensity ratios are close to the nominal composition. The 1000 °C annealed sample shows, by contrast, an increased 0.37 intensity ratio thus indicating that some Bi oxide has segregated to the surface.[53,54] This latter result is in tune with the yellowish color of the 1000 °C annealed sample.

SEM micrographs provide indication on the particle size even though, of course, they cannot be diagnostic of any particular crystalline phase. Figure 6 shows micrographs of a representative 10% Bi-doped sample, fired at 200 and 1000 °C. There is evidence of a remarkable dependence of the sample morphology of the annealing temperature as inferred from XRD data (Table 2). In particular, larger crystalline agglomerates are formed upon increasing the firing temperature. The sample morphology dramatically changes at 1000 °C where a high crystallinity is achieved and the monoclinic phase becomes predominant. It is worth noting that the sizes of small particles are in good agreement with those measured from the diffraction data (Table 2), even though the presence of larger crystals indicates that some agglomeration mechanism is obviously operating.

Conclusion

The coprecipitation of Bi and Zr as a hydroxide gel followed by annealing in air at temperatures ranging from 400 to 800 °C stabilizes zirconia in tetragonal phase.

XRD and Raman spectra point to the tetragonal symmetry of the present Bi-doped samples. The presently observed novel stabilization by Bi^{3+} ions, is tuned with other studies,[2,5,12,32,54−62] even though it contrasts the previously proposed model which suggests that only cations more ionic than Zr can be capable of stabilizing effects in zirconia.[28] The XPS spectra reveal the presence of Bi(III) and of a small amount of a lower Bi oxide. Progressive heating treatments of Bi-doped ZrO_2 cause surface segregation of the Bi oxide which separates from the tetragonal phase, thus leaving the thermodynamically more stable monoclinic ZrO_2.

Finally we must mention that the interesting surface composition of the present systems deserves enough motivation for further surface investigations.

Supporting Information Available: X-ray powder diffraction patterns, over a $20° < 2\theta < 80°$ angular range, for undoped ZrO_2 (1 page). Ordering information is given on any current masthead page.

Acknowledgment. I.F. and A.G. thank the CNR (Rome) for financial supports.

CM950558J

(50) DharmadhiKari, V. S.; SainKar, S. R.; Badrinarayan, S.; Goswami, A. *J. Electron Spectrosc. Relat. Phenom.* **1982**, *25*, 181.
(51) Morgan, W. E.; Stec, W. J.; Van Wazer, J. R. *Inorg. Chem.* **1973**, *12*, 953.
(52) Briggs, D.; Seah, M. P. *Practical Surface Analysis*, 2nd ed.; Wiley: Chichester, 1994.
(53) Hughes, A. E. *J. Am. Ceram. Soc.* **1995**, *78*, 369.
(54) Kim, Y. H.; Kim, H. G. *J. Mater. Sci.: Mater. Electron.* **1994**, *5*, 260.
(55) Kim, D. J.; Jung, H. J.; Cho, D. H. *Solid State Ionics* **1995**, *80*, 67.
(56) Kim, D. J.; Jang, J. W.; Jung, H. J.; Hug, J. W.; Yang, I. S. *J. Mater. Sci. Lett.* **1995**, *14*, 1007.
(57) Hartmanova, M.; Travenec, I.; Urusovskaya, A. A.; Putyera, K.; Tunega, D. *Solid State Ionics* **1995**, *76*, 207.
(58) Dravid, V. P.; Ravikumar, D.; Notis, M. R.; Lyman, C. E.; Dhalenne, G.; Revcolevschi, A. *J. Am. Ceram. Soc.* **1994**, *77*, 2758.
(59) Hartmanova, M.; Poulsen, F. W.; Hanic, F.; Putyera, K.; Tunega, D.; Urusovskaya, A. A.; Oreshnikova, T. V. *J. Mater. Sci.* **1994**, *29*, 2152.
(60) Fukuya, M.; Hirota, K.; Yamaguchi, O.; Kume, H.; Inamura, S.; Miyamoto, H. *Mater. Res. Bull.* **1994**, *29*, 619.
(61) Feng, M.; Goodenough, J. B. *J. Am. Ceram. Soc.* **1994**, *77*, 1954.
(62) Naito, H.; Arashi, H. *Solid State Ionics* **1994**, *67*, 197.